Application of a mineral binder to reduce VOC emissions from indoor photocatalytic paints

Julien Morin, Adrien Gandolfo, Brice Temime-Roussel, Rafal Strekowski, Gregory Brochard, Virginie Bergé, Sasho Gligorovski, Henri Wortham

Application of a mineral binder to reduce VOC emissions from indoor photocatalytic paints

Julien Morin[a,*], Adrien Gandolfo[a], Brice Temime-Roussel[a], Rafal Strekowski[a], Gregory Brochard[b], Virginie Bergé[b], Sasho Gligorovski[c], Henri Wortham[a,*]

[a] Aix Marseille Univ, CNRS, LCE, UMR 7376, 13331 Marseille, France

[b] ALLIOS, Les Docks Mogador, 105 chemin de St Menet aux Accates, 13011 Marseille, France

[c] State Key Laboratory of Organic Geochemistry, Guangzhou Institute of Geochemistry, Chinese Academy of Sciences, Guangzhou 510 640, China

[*] Corresponding authors: e-mail: henri.wortham@univ-amu.fr, Phone: +33 413551039

E-mail: julien.morin@univ-amu.fr; Phone: +33 647308629

ABSTRACT

Given toxic nature of many volatile organic compounds (VOCs) present within indoor environments, it is necessary to measure and quantify indoor VOC emissions to better inform and protect the public from possible adverse health effects of indoor air pollution. To better understand and quantify this problem, a horizontal flow tube reactor was used to study VOC emissions from selected paint. Studied paints include mineral silicate binders, acrylic binders and acrylic/siloxane binders with and without incorporated titanium dioxide (nano-TiO_2) nanoparticles. Surface emission fluxes of selected VOCs from the tested paints were detected and quantified using a High Sensitivity-Proton Transfer Reaction-Mass Spectrometry (HS-PTR-MS). Low VOC emissions were observed for reference paints (absence of nano-TiO_2) in

the presence of UV irradiation. On the other hand, important formation of formaldehyde, acetaldehyde and pentanal were observed for photocatalytic paints (impregnated with nano-TiO_2). VOC emission fluxes from reference paints and photocatalytic paints were compared to determine the formation of VOCs due to a reaction between the binder and radical reactive species created on photocatalytic surfaces. Different matrix impacts for each paint were studied and an important difference in VOC emission between acrylic binder paints and mineral binder paints was observed under UV irradiation. A 66%, 29% and 88% decreases in formaldehyde, acetaldehyde and pentanal, respectively, emission were observed for mineral binder compared to acrylic binder VOC emission. In majority of the experiments, mineral binder emitted less VOCs compared to acrylic binder. This mineral binder seems to be an important factor in improving indoor air quality.

Keywords: Indoor Air; Formaldehyde; Photocatalytic Paints; VOC emissions; Surface emission fluxes

1. INTRODUCTION

It is now well recognized that private residences, schools and commercial buildings among others are important environments of human exposure to air pollutants[1]. In the modern world, an average human spends over 90% of her/his lifetime within indoor settings[2]. Numerous compounds that include nitrous acid (HONO)[3], particulate matter (PM), carbon monoxide (CO), nitrogen oxides (NOx) and volatile organic compounds (VOCs) are known to be ubiquitous indoor air pollutants[4,5]. Some VOCs are known to cause adverse human health effects because they are easily absorbed through skin and/or mucous membranes[6,7]. Based on a study carried out by the United States Environmental Protection Agency (U.S. EPA)[2], the VOC levels within indoor environments in US are typically 5 to 10 times higher than those of outdoor settings. Further, it has been observed that within Chinese homes, the indoor VOCs levels are 100 to 1000 times higher compare to European home environment[8]. Indoor VOC sources are numerous and include emissions from building materials, combustion processes, furnishing or household products. Recently, Geiss *et al.*[9] studied indoor (offices, schools, private homes) and outdoor environment emissions of selected VOCs across Europe to calculate their indoor-to-outdoor environment concentration ratios. These investigators calculated the work to school environment ratios of 21 VOCs that included BTEX compounds (namely, benzene, toluene, ethylbenzene, xylenes) and aldehydes (namely, formaldehyde and acetaldehyde among others) to range from 1.2 to 14.3. The results of Geiss *et al.*[9] imply point sources of VOCs within indoor settings since the ratio indoor-to-outdoor environment ratio > 1 indicates higher VOC concentrations within indoor environments than outdoors. In France[10], similar work has been performed in low-energy buildings, representative of future building designs and constructions. In a simulation similar to the one listed above, the calculated indoor-to-outdoor ratios were > 1 meaning that health risks for indoor environment occupants will remain a major occupational concern well into the future.

To better improve indoor and outdoor air quality, different nano-TiO_2 particle based photocatalytic paint materials continue to be developed. In the environmental remediation of atmospheric pollutants, nano-sized TiO_2 photocatalyst was chosen because of its superior photocatalytic oxidation potentials, non-toxic properties, low price and anti-photocorrosive properties[11] compared to other heterogeneous photocatalytic methods or photoelectrochemical phenomena used in the building and construction industry.

To date, a majority of small scale laboratory and larger scale chamber[12] experimental studies have concentrated their research effort to study the photocatalytic consumption and/or degradation of NOx [13–17] (NOx = NO + NO_2) and VOC [18–21] pollutants on selected photocatalytic materials. Fewer studies have been reported in the literature that researched VOC emissions from the photocatalytic paint materials themselves[9,21–23]. However, it has been proposed that the binder molecules present within the paint may react with reactive radical species, namely, OH radicals, present on nano-TiO_2 surfaces in the presence of light to emit VOCs, therefore, act as a point source of atmospheric pollutants[9,21–23]. This is troublesome since practically all paint materials contain various amounts of organic binder matter or a solvent, that is, all paints include some sort and quantity of a binder because it is the binder itself that keeps the pigment in place after the paint dries. In fact, an important increase in acetaldehyde and formaldehyde emissions from photocatalytic paints under UV irradiation have been observed[21,23]. Other compounds that include ethylacrolein, pentanal, 1-hydroxy-butanone and hexanal have also been detected[21]. As a result, the photocatalytic reactions that lead to VOC emissions from wall paints are important because they may affect the durability of the paint, limit its photocatalytic properties and have direct and/or indirect impacts on human health, human well-being and indoor air quality. Further, the photocatalytic degradation of the binder matrix may significantly reduce the advantages of this technology. Consequently, to limit VOC emissions within indoor environments from the photocatalytic

degradation of the binder matter present in the photocatalytic paints, a new generation of binders is being developed.

In this work, three binder matrices were investigated for possible photocatalytic VOC emissions. The surface emission fluxes were measured for binders with and without nano-sized TiO_2 particles. Initial experiments were realized under "dark" conditions, that is, in the absence of UV irradiation, to better quantify any VOC emissions due to the inherent paint chemical composition. Other experiments were carried out in the presence of UV light to see if the presence of nano-sized TiO_2 particles plays an effect on the surface emission fluxes. The obtained results for mineral silicate and acrylic/siloxane binders are compared with acrylic binder to determine any possible impacts and effects of the paint composition. The obtained results will help to improve the binder formulation materials to minimize any photocatalytic VOC emissions from photocatalytic paints.

2. MATERIALS AND METHODS

2.1. Preparation of paints

All paints were formulated and produced by the local paint manufacturer ALLIOS (Marseille, France). Three different binder pairs studied include (1) copolymer acrylic (mix butyl acrylate and vinyl acetate), (2) a copolymer acrylic/siloxane and (3) mineral silicate. Each binder pair included (1) one photocatalytic binder (P) that contained nano-sized TiO_2 particles and (2) one reference paint (R) without any nano-sized TiO_2 particles present in the binder. All mineral binders contained 5% of the organic binder to help the drying process of the selected paint on the given support so that only non-volatile content of a paint remained after the coating solidifies. Binder compositions are shown in Table 1.

Table 1: Composition of selected binders evaluated in this work. Binder with (+) and without (-) a photocatalytic component.

Name	Binders	Photocatalytic

		Component
P1	Acrylic copolymer + TiO_2	+
R1	Acrylic copolymer	-
P2	Acrylic copolymer /siloxane (60/40) + TiO_2	+
R2	Acrylic copolymer /siloxane (60/40)	-
P3	Mineral silicate + TiO_2	+
R3	Mineral silicate	-

The paints were applied on one side of glass plates that were 30 cm long and 2 cm wide according to a standard operating procedure developed by the manufacturer ALLIOS[17]. This procedure allowed for production of homogeneous, uniform and reproducible wet films that were 100 µm thick. The painted glass plates were stored for 21 days at T=298 K while a humidified (55% RH) synthetic air was allowed to flow over the plates. Two types of TiO_2 particles were used: (1) the larger sized ultrafine (micro-size) TiO_2 powder was used to render the paints whiter and (2) the nano-sized TiO_2 particles were used to render the paints photoactive. All photocatalytic paints contained the TITANE P2 white pigment in anatase form. The nano-sized TiO_2 particle content was 85% and the ultrafine (micro-size) TiO_2 powder had a listed specific area of 350 $m^2 g^{-1}$. All photocatalytic paints contained 13.4% (w/w) of the inactive micro-size TITANE P2 particles. A mixture of ground additives (slurry), was prepared with 35% (w/w) active nano-sized TiO_2. Then, other paint constituents (architectural constituent of paints, i.e.,$CaCO_3$ and micrometric TiO_2) was mixed with 10% of the slurry to reach 3.5% (w/w) of photocatalytic active TiO_2 nanoparticles.

2.2. Experimental setup

The flow tube reactor used in this work is similar to the one used in previous studies of VOC emissions from photocatalytic paints[17,23]. Here, the horizontal flow tube reactor experiments involved time-resolved detection of the selected VOCs emitted from the solid paint media using the High Sensitivity-Proton Transfer Reaction-Mass Spectrometry (HS-PTR-MS)

(IONICON Analytik, Austria) in the presence of UV irradiation or under "dark" conditions, that is without UV light irradiation.

The schematic diagram of the apparatus has been published elsewhere[23,24] and is described in detail in Figure S1. Some experimental details that are particularly relevant to this work are given below.

A borosilicate glass double-wall horizontal flow tube reactor with an internal volume of approximately 131 cm^3 was used to study surface VOC emission fluxes of selected solid paints as a function of given experimental conditions. The flow tube reactor was maintained at a constant temperature (±1 K), using a RC6 LAUDA temperature-controlled circulating bath, by allowing water to circulate through the outer jacket. All experiments were carried out at T=(298±1) K and at 1 atm total pressure of synthetic air (Linde Gas, >99.999 stated purity). The geometry of the flow tube reactor was such that it allowed for the synthetic air carrier gas flow to enter at one end and the High Sensibility Proton-Transfer Reaction-Mass Spectrometer (HS-PTR-MS) (IONICON Analytik) to be located downstream at the opposite end. Similar to the work of Hanson and Ravishankara[25], the flow tube was mounted horizontally, and the paint was applied on a glass plate located within the flow tube. The plate was made of glass and was 30 cm long and 2 cm wide.

The flow tube reactor was placed within a stainless-steel protective box. Within the box, two UV fluorescent lamps (Philips TL-D 18W Actinic BL, 340-400 nm, λ_{max} = 368 nm, length = 60 cm) were placed side-by-side on the upper side of the reactor. A stainless-steel box was used because stainless-steel exhibits good reflection properties and allows for a homogeneous irradiation during experiments. The spectral irradiance of the UV lamps used in this work has been determined previously[26] and was estimated to be 8.5 W m^{-2}. This value represents a mean integrated irradiance, ($340<\lambda(nm)<400$), of solar light that is known to

enter an indoor environment[26]. A sheath of synthetic air flow (300 sccm) was allowed to enter the flow-tube system. This flow was controlled using a mass flow controller (Brooks SLA Series mass flow controller, in the range 0–1 slm, ±1% stated accuracy). Dimensions and geometry of the flow reactor and the experimental conditions allowed for the experiments to be carried out at laminar flow conditions. The flow rate through the reactor was 1.1 cm s^{-1} and the residence time was 27 seconds. Prior to allowing the synthetic air to enter the flow tube reactor, the air flow was separated into two separate flows, one of dry air and the other humidified by bubbling in deionized water (resistivity >18 MΩ cm). Deionized water was prepared by allowing tap water to pass through a reverse osmosis demineralization filter (ATS Groupe Osmose) followed by a commercial deionizer (Millipore, Milli-Q50). Gas flows were controlled using needle valves and the relative humidity could be changed by varying throughput of these valves. Finally, the two flows were allowed to mix to obtain an experimental relative humidity (RH) of 40%. The RH was measured online at the reactor exit using a hygrometer "Hygrolog NT2" (Rotronic) with "HygroClip SC04" probe. The accuracy of RH measurements was ±1.5%. More details on the experimental setup is available in the Supporting Information (Figure S1).

2.3. VOCs measurements

It is now well recognized, that Proton Transfer Reaction-Mass Spectrometry (PTR-MS) technology is an excellent technique to measure rapid changes in gas phase concentration of selected VOCs[23]. In this work, an HS-PTR-MS system was used to carry out online measurements of VOC emissions. This technique was previously described in detail elsewhere[27]. Briefly, it consists of an electron impact in ion source that produces hydronium ions, H_3O^+, that react with the neutral organic molecule, R, within the drift tube to produce water and the pseudo-molecular ion, $[RH]^+$, as show below:

$$H_3O^+ + R \rightarrow H_2O + RH^+$$

This reaction is only possible if the proton affinity of R is higher than the proton affinity of H_2O. The resulting ion products are then mass selected and detected using the electron multiplier detector.

The HS-PTR-MS was operated with a drift pressure and a temperature of 2.02 mbar and 333 K respectively. The drift voltage was 500 V that corresponded to the E/N value of 124 Townsend (1 Townsend = 10^{-17} V cm^2), where E is the electric field (V cm^{-1}) and N is the ambient air number density within the drift tube (cm^{-3}). The quantification of VOCs was based on calibration with certified gas containing different mixtures of aromatic hydrocarbons at 100 ppb levels (RESTEK 34423-PI).

The VOC emissions were analyzed in a full mass spectrum mode between 21 and 200 amu and the detection rate was 1 s amu^{-1}. The resulting HS-PTR-MS time resolution was 3 min.

2.4. VOCs mixing ratio and estimation of surface emission fluxes

The VOC mixing ratio (ppb) was calculated using the following equation [28]:

$$C_x = 1.65 \times 10^{-11} \times \frac{U_{drift} \times {T_{drift}}^2}{k \times {P_{drift}}^2} \times \frac{i[X]}{i[H_3O^+] + Xr \times i[H_3O^+(H_2O)]} \quad (1)$$

where X is the target compound, H_3O^+ and $H_3O(H_2O)^+$ are the reagent ions. i[X], i[H_3O^+] and i[$H_3O^+(H_2O)$] are the ion signals in counts per second (cps) of X, H_3O^+ and $H_3O(H_2O)^+$, respectively, normalized by their corresponding transmission efficiencies; U_{drift} is the drift tube voltage (V); T_{drift} is the drift tube temperature (K); k is the proton-transfer reaction constant (cm^3 s^{-1}); P_{drift} corresponds to the pressure within the drift tube (mbar).

The *m/z* specific relative transmission efficiency was experimentally determined over the mass range of 21-181 with a calibration gas standard, consisting of a mixture of 14 aromatic organic compounds (TO-14A Aromatic Mix, Restek Corporation, Bellefonte, USA, 100±10 ppb in Nitrogen).

The factor Xr is compound specific and has been described previously[29]. This factor reflects both the difference in the rate coefficient for the proton-transfer-reactions H_3O^+ + R and $H_3O(H_2O)^+$ + R and the difference in transmission efficiencies for the two reagent ions of the quadrupole mass spectrometer. These values were directly taken from the works of de Gouw *et al.*[29] and Gandolfo *et al.*[23]. When no value was available in the literature, Xr= 0.5 was used as recommended by de Gouw *et al.*[29].

The values of k have been determined elsewhere[30,31] and when no proton-transfer-reaction rate constant value for the compounds of interest were available in the literature, the canonical $k= 2 \cdot 10^{-9}$ cm^3 s^{-1} value was used. The k and Xr values used in this work are shown in Table S1 in the Supporting Information.

The HS-PTR-MS is known to underestimate the concentration of formaldehyde[32]. Therefore, a correction factor of 2.7 was used to obtain the global quantity of this VOC. The correction factor was previously determined in the laboratory setting and the experimental procedure is detailed in the Supporting Information of Gandolfo *et al.*[23].

The surface emission fluxes (molecules cm^{-2} s^{-1}) for different compounds were determined using the following equation:

$$\text{Surface Emission Fluxes X} = \frac{C_x \times 2.46 \times 10^{10} \times \text{Internal reactor volume}}{(\text{Residence time} \times \text{Paint surface})} \quad (2)$$

Where the internal reactor volume, the residence time within the reactor and the paint surface are expressed in cm^3, s, cm^2, respectively. C_x is the mixing ratio (ppb) measured at the exit of the reactor as a function of time for the target compounds. 2.46×10^{10} is the conversion used to convert ppb to molecule cm^{-3}.

3. RESULTS AND DISCUSSION

3.1. VOCs identification

The identification of selected VOCs was based on mother-ion masses weight, fragmentation fingerprints, bibliography and previously published data. Given the HS-PTR-MS instrument used in this work, certain mass to charge ratios, namely *m/z* 33, 45, 57, 59, 61, 67, 71, 79, 89, 107, 121 and 123 were easily attributed to specific VOC compounds. However, identification of eight ions, namely *m/z* 47, 57, 71, 73, 75, 87, 89 and 129 could not be easily attributed to a specific compound. However, earlier laboratory[23] of P1 and R1, using the Proton Transfer Reaction-Time of Flight-Mass Spectrometry (PTR-ToF-MS) attributed *m/z* 47, 57, 71, 73, 75, 87, 89 and 129 as formic acid, acrolein, methyl vinyl ketone (MVK), acrylic acid, propionic acid, pentanal and/or vinyl acetate, propionic acid and octanal, respectively. As a result, the above listed seventeen *m/z* ratios were chosen to identify and quantify the selected VOCs used in this work (see Table 2).

The formaldehyde, acetaldehyde and benzene emission results are shown individually because these compounds are known to cause adverse health effects. The other VOCs have been grouped as a function of their chemical class. The chemical classes of the selected compounds are shown below in Table 2.

Table 2: Compounds detected and quantified using the HS-PTR-MS technique. References : (a) Manoukian *et al.*[33], (b) De Gouw *et al.*[29], (c) Karl *et al.*[34], (d) Hartungen *et al.*[35], (e) Jobson *et al.*[36], (f) Gandolfo *et al.*[23].

Most probable compound	*m/z*	Chemical classes	Ref
Formaldehyde	31		a, c
Methanol	33		b, c, e
Acetaldehyde	45		a, b, c, e
Formic Acid	47	Acids	c
Acrolein	57	Carbonyls	c
Acetone + Propanal	59	Carbonyls	a, b, c, e
Acetic Acid	61	Acids	b, c, d, e
Methyl Vinyl Ketone	71	Carbonyls	b, c
Acrylic Acid	73	Acids	f

Propionic Acid	75	Acids	d
Benzene	79		a, b, c, e
Pentanal + Vinyl Acetate	87	Carbonyls	a, f
Butanoic Acid	89	Acids	d
Ethylbenzene + Xylene	107	Aromatics	a, b, c
Trimethylbenzene + Ethyltoluene	121	Aromatics	a, b, c
Benzoic Acid	123	Aromatics	e, f
Octanal	111 and 129	Carbonyls	f

3.2. Typical Experiment

In a typical experiment, the studied paint on its glass support was placed in the horizontal flow tube reactor and was left in the "dark" (UV lamps off) for two hours (T_0). Here, the nano-TiO_2 particles present in the photocatalytic paint were not activated and the "dark" VOC emissions were determined. After, the UV lights were turned on for three hours (T_1). Here, the photocatalytic paints were activated and the formed reactive radicals species reacted with the organic compounds present in the binder which leading to VOC formation[9,22,23]. Finally, UV lights were turned off (T2) and the VOC emission signal was followed for another two hours. A typical example of the formaldehyde temporal profile is shown in Figure 1. The observed ion temporal profile is the same for all VOCs used in this work.

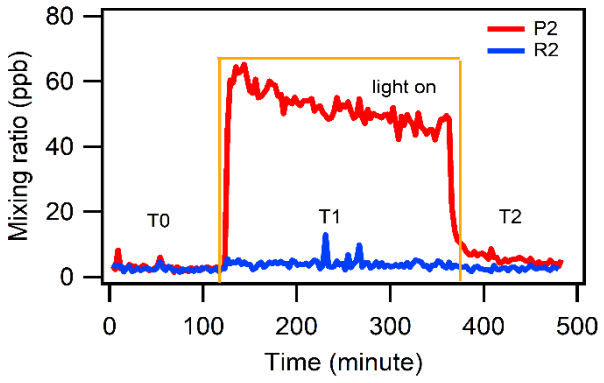

Figure 1: Typical temporal profile of formaldehyde emission from P2 (red line) and R2 (blue line) at T=298 K and RH=40%.

The observed formaldehyde temporal profiles obtained for photocatalytic (P2) and reference (R2) paint are different. For R2, when the UV light is turned on, a very slight increase in the formaldehyde temporal profile signal is observed and when the UV light is turned off, the ion signal comes back to its original base value.

For P2, when the UV light is turned on the formaldehyde ion signal increases significantly. Here, in a time frame of a few minutes the formaldehyde ion signal stabilizes and remains nearly constant for the rest of the irradiation period (T1). Once the UV lamps are turned off, the intensity of the formaldehyde ion signal drops immediately and reaches its initial value within few minutes.

3.3. Surface Emission Fluxes

3.3.1. Reference paints

The VOCs surface emission fluxes of reference paints (R1, R2 and R3) under (1) "dark" condition (lozenge) and (2) under UV light (solid) are shown in Figure 2.

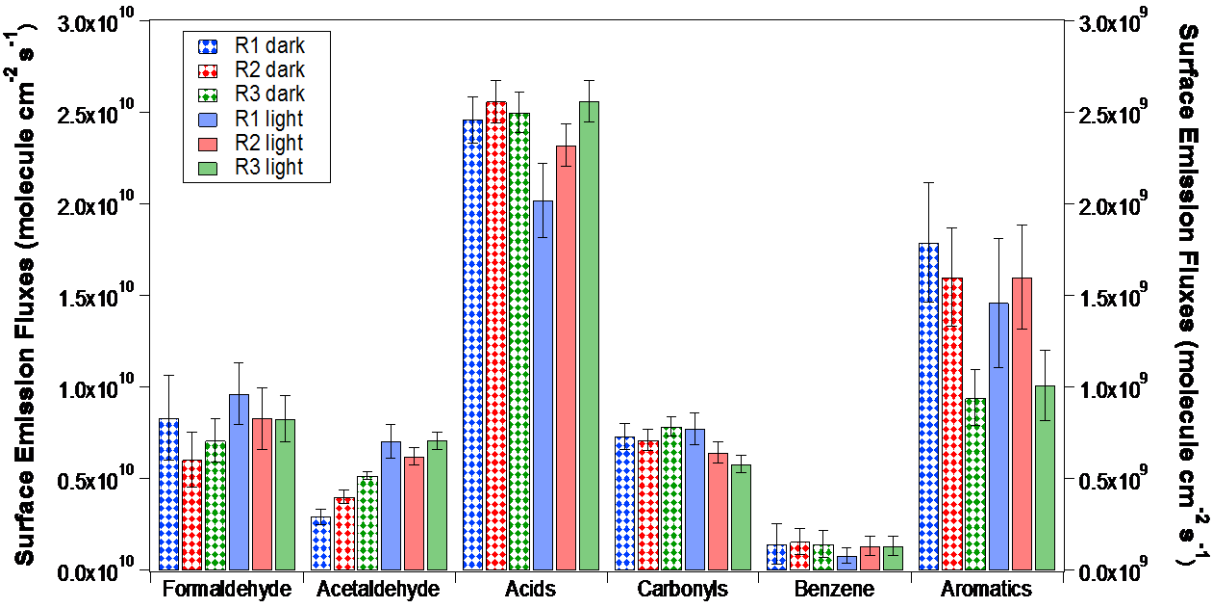

Figure 2: VOCs surface emission fluxes (molecule cm^{-2} s^{-1}) obtained for selected compounds under "dark" conditions (lozenge) and in presence of UV light (solid). Surface emission fluxes for formaldehyde, acetaldehyde, acids and the carbonyls are shown on the left axis, aromatics and benzene on the right axis. Blue bars correspond to R1, red bars to R2 and green bars R3. Errors bars are ±1σ precision based on ten experimental point values.

As shown in Figure 2, the surface emission fluxes of R2 and R3, were compared to R1 under "dark" conditions. For most compounds, the difference in surface emissions fluxes were inferior to 25% but in some cases an important difference was observed. For example, an increase of 37% for R2 and 77% for R3 in the acetaldehyde surface emission fluxes, have

been observed. The selected acids surface emission fluxes seem to be analogous for the three binders. However, increases of 37% in acrylic acid, R2, and 39%, R3, in propionic acid emissions have been observed. Other acids' surface emission fluxes are similar or decrease down to 27% (formic acid R3). Moreover, for R3, decreases in aromatics' emissions have been observed. This decrease is mainly due to 64% and 73% decrease in ethylbenzene and benzoic acid emissions, respectively. In general, the surface emission fluxes values were in the same range. Even though an observed maximum difference of 77% in emission fluxes was observed under "dark" conditions the influence of binder composition on VOC emissions is very low when the paint surfaces are not exposed to UV radiation. All surface emission fluxes are shown on tables S2-S4 in Supporting Information.

The VOCs emissions under "dark" conditions were compared with those under UV light. As shown in Figure 2, the most important variation was observed for acetaldehyde; emission increases of 142% for R1, 55% for R2 and 37% for R3 have been measured under "light" conditions compared to experiments carried out under "dark" experimental conditions. The emissions of acids are observed to be similar under "dark" and "light" conditions. An exception is the acrylic acid. Here, acrylic acid emission increases of 56% and 45% have been measured for R1 and R2, respectively. On the other hand, a decrease of 12% in formic acid emission and 29% in the acetic acid emission for R1 as well as a decrease of 12% in acetic acid and formic acid emissions for R2, have been observed.

The surface emission fluxes of carbonyls compounds by R1 are, globally, similar even if the emission of pentanal increase of 38% has been observed. Regarding R3, a decrease of carbonyls emission has been observed due to 38% reduction in acetone emission. As shown in Figure 2, a decrease of 44% of benzene emission by R1 has been observed.

With respect to the aromatics, an increase in 56% of benzoic acid emission has been observed by R3 even if the global emission for this class of compounds is similar. For the rest of the compounds, the difference in emission is inferior to 25%. All surface emission fluxes are shown on tables S2-S4 in Supporting Information.

The obtained results show that near-UV light has a low impact on the VOCs surface emission fluxes from reference paints. Moreover, emission fluxes are similar for the three binders, that is, inferior to 25%, for most emissions, for the three binders under "dark" and under UV irradiation. Here, the binder composition has no impact on VOC emissions implying that a limited impact of the selected reference paints on indoor air pollution.

3.3.2. Photocatalytic paints under "dark" and UV light conditions

In this part, the surface emission fluxes of formaldehyde, acetaldehyde, benzene, aromatics, acids and carbonyls were studied under "dark" conditions and UV irradiation for the three photocatalytic paints (P1, P2 and P3). The obtained emissions results from photocatalytic paints under "dark" and UV light experimental conditions are shown in Figure 3.

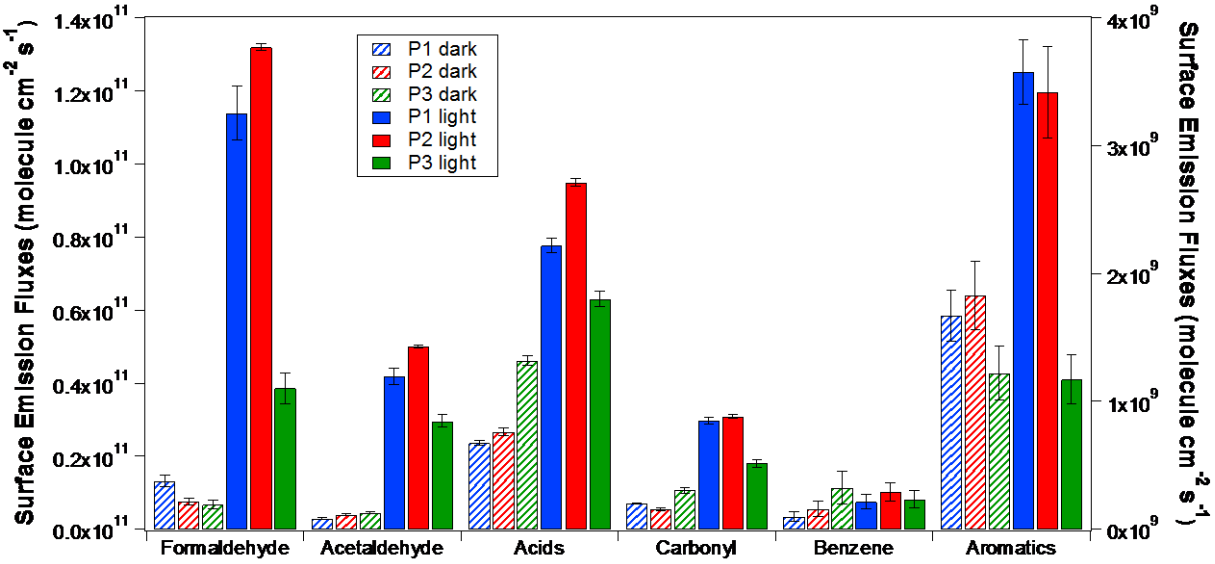

Figure 3: VOCs surface emission fluxes (molecule cm^{-2} s^{-1}) obtained for different compounds under "dark" (hatched) conditions and under UV irradiation (solid). Surface emission fluxes for formaldehyde, acetaldehyde,

acids and carbonyls are shown on the left axis, aromatics and benzene on the right axis. Blue bars correspond to P1, red bars to P2 and green bars to P3. Errors bars are ±1σ, precision based on ten experimental point values.

As shown in Figure S3, a comparison of the surface emission fluxes between photocatalytic paints and reference paints under "dark" conditions shows an increase of 130% for benzene and 83% for benzoic acid for P3. However, the VOC emissions from both photocatalytic and reference paints are observed to be in the same concentration range. This implies that the presence of nano-TiO_2 particles in the binder does not affect the VOC emissions under "dark" conditions.

Further, VOC surface emission fluxes by P1, P2 and P3 under "dark" conditions are shown in Figure 3. For formaldehyde, emissions have been observed to decrease 43% and 49% for P2 and P3, respectively. On the other hand, acetaldehyde emissions are observed to increase 37% for P2 and 58% for P3.

The P3 surface emission flux of all acids under "dark" experimental conditions, increased by 95% compared to P1 surface emission flux. This emission increase has been observed to correspond mainly to acetic acid and propionic acid emission, +219% and +131%, respectively. An increase of 88% in acetone emissions have been observed for P3 but the global emission of carbonyl compounds is similar for both types of paints. This compensation is due to an observe decrease by 15% of MVK and pentanal surface emission fluxes. An important difference is observed in the emission of benzene; an increase of 65% for P2 and 237% for P3 has been observed. Finally, aromatic compounds surfac0e emission fluxes have been observe to decrease 33% for P3, an effect compounded by an0 induced benzoic acid emission decrease of 48%. For the remaining VOCs, the difference of the emission fluxes between the two binders is smaller than 30%. All surface emission fluxes are shown on tables S5-S7 in Supporting Information.

Although P3 are observed to release 32% more VOCs compared to P1 and 44% more than P2 under "dark" conditions, this difference is negligible compared to the difference in emissions under UV light experimental condition for photocatalytic paints. Therefore, it can be concluded that the composition of the binder has a limited impact on VOC emissions under "dark" conditions.

In the presence of UV light, the difference in surface emission fluxes was observed to be more important compared to the experiments carried out under "dark" conditions as details below.

In addition to experiments carried out under "dark" conditions, the surface emission fluxes by P1, P2 and P3 were also evaluated in the presence of UV radiation ($340 < \lambda(nm) < 400$, $\lambda_{max} = 368$ nm, 8.5 W m^{-2}). For R3, a decrease of 66% in formaldehyde, 29% in acetaldehyde, 40% in all carbonyl and 68% in all aromatic compounds emission as compared to P1 have been observed. As shown in Figure 3, the selected compound emissions for P2 (red bars) and P1 (blue bars) seem similar or at least within the shown error bars. However, it was not possible to differentiate the individual emissions of selected VOCs in Figure 3. Emission impact from P2 and P3 compared to P1 emission will be discussed later for individual VOCs (Table 3).

All surface emission fluxes for each compound under different experimental conditions are shown in the Supporting Information (Table S5-S7).

The impact of each binder on VOCs emission was evaluated in order to find out the best performance of the photocatalytic paints as a remediation technology aimed to clean the air in indoor environments.

As shown in Table 3, the selected VOC emissions from P2 and P3 are compared to P1, under UV light experimental conditions.

Table 3: Surface emission fluxes of selected VOCs for P2 and P3 as compared to the VOC emissions observed for P1. Standard deviations are precision only and are based on ten experimental point values.

Compounds	P1 surface emission fluxes (molecule cm^{-2} s^{-1})	P2	P3
Formaldehyde	$(1.14\pm0.07)\cdot10^{11}$	+16%	-66%
Methanol	$(2.02\pm0.15)\cdot10^{10}$	-7%	-41%
Acetaldehyde	$(4.18\pm0.22)\cdot10^{10}$	+20%	-29%
Formic Acid	$(1.13\pm0.05)\cdot10^{10}$	+7%	-27%
Acrolein	$(7.15\pm0.65)\cdot10^{9}$	+13%	-17%
Acetone + Propanal	$(1.30\pm0.07)\cdot10^{10}$	-14%	-25%
Acetic Acid	$(2.58\pm0.15)\cdot10^{10}$	+32%	+27%
Methyl Vinyl Ketone	$(1.35\pm0.14)\cdot10^{9}$	+3%	-66%
Acrylic Acid	$(2.29\pm0.09)\cdot10^{10}$	+40%	-94%
Propionic Acid	$(6.46\pm0.44)\cdot10^{9}$	+25%	+198%
Benzene	$(2.15\pm0.59)\cdot10^{8}$	+36%	+7%
Pentanal + Vinyl Acetate	$(6.39\pm0.27)\cdot10^{9}$	+26%	-88%
Butanoic Acid	$(1.13\pm0.09)\cdot10^{10}$	-23%	-88%
Ethylbenzene + Xylene	$(1.81\pm0.18)\cdot10^{9}$	-21%	-73%
Trimethylbenzene + Ethyltoluene	$(1.53\pm0.17)\cdot10^{9}$	+10%	-73%
Benzoic Acid	$(2.41\pm0.57)\cdot10^{8}$	+26%	-45%
Octanal	$(1.83\pm0.28)\cdot10^{9}$	+20%	-45%
Total Emission	$\mathbf{(2.87\pm0.08)\cdot10^{11}}$	**+15%**	**-43%**

It can be seen (Table 3), that the net VOC emission flux of selected compounds from P2 are 15% higher as compared to the VOC emission flux from P1. The observed positive net difference in the total emission between the two paints is probably best explained by the difference in the composition or formulation of the paint binders. That is, in the paint composed of the acrylic/siloxane binder, only 40% of the copolymer acrylic was replaced by siloxane, R_2SiO, that still contains an organic group, R. As a result, the observed change in the VOC emission flux between these two paints has no positive impact on indoor air quality. Therefore, the acrylic/siloxane binders are of little interest to mitigate human health risks from indoor air pollution.

On the other hand, the net VOC emission flux of selected compounds from P3 under UV irradiation was 43% lower as compared to VOC emissions from P1. As shown in Table 3, majority of surface emission fluxes of selected VOCs from P3 are lower as compared to the

VOC emissions from P1 except for propionic acid (+198%), and acetic acid (+28%). The limited emission VOC fluxes are likely due to the organic compound that is still present in the mineral silicate binder. In other cases, we observed a large decrease of up to -88% for pentanal and butanoic acid, as compared to P1. It may be supposed that if the photocatalytic paints are formulated without any organic compounds mixed within the binder, the VOCs emissions will be eliminated. However, to date, it is not possible to produce paints without any organic matter present in the binder. It is necessary to have at least 5% of the organic binder to obtain a good drying on the given surface support. Nevertheless, this mineral binder seems to be an important innovation and a possible mitigation strategy to improve the indoor air quality by considerable reduction in the VOC emissions from paints containing mineral binder as compared to more traditional organic paints used in the past.

3.4. Environmental Implications

Sources of indoor VOCs are numerous that include emissions from building materials (wood, PVC pipes), combustion processes (e.g. cooking), furnishing (carpets[37], floor coverings[38]) or utilization of household cleaning products[39–41].

Based on the experimental results obtained in this work, we estimated the formation of a harmful indoor air pollutant, i.e., formaldehyde in a model room. For the model calculations, we considered a room that is 2.5 m high, 5 m wide and 4 m long; hence a total volume of 50 m^3 with floor covering[38], carpets[37], sofa[42], furniture[43]. In order to simulate more realistic living conditions, we considered that only 4 m^2 of the wall is irradiated with direct sunlight of 8.5 W m^{-2} for in the wavelength region between 300 and 400 nm [26,44] at 298 K and 40% RH.

The elimination rate constant (k_{obs}) corresponds to the sum of air exchange rate and the removal process rate. Considering an average air exchange rate of 0.56 h^{-1} [(45)] and removal

process rate of 1.01 h^{-1} [33], we obtained an elimination rate constant of 1.57 h^{-1}. The removal process encompasses the reactivity, surface adsorption, phase change and decomposition.

Moreover, we assumed a constant production of formaldehyde under direct light irradiation. The formation of formaldehyde is calculated using the following equation[33]:

$$C_a(t) = \frac{E_R}{k_{obs}V} + \left(C_0 - \frac{E_R}{k_{obs}V}\right) e^{(-k_{obs}t)}$$

where $C_0 = 0$, is the initial formaldehyde concentration (mg m^{-3}), $C_a(t)$ is the formaldehyde concentration **at** time (mg m^{-3}), E_R is the formaldehyde mass emission rate induced by photocatalytic paint (mg h^{-1}), k_{obs} is the elimination rate constant (h^{-1}) and V is the total volume of the room (50 m^3).

In Figure 4, we can see the calculated formaldehyde emission mixing ratio within the room from various photocatalytic paints in the presence of UV light.

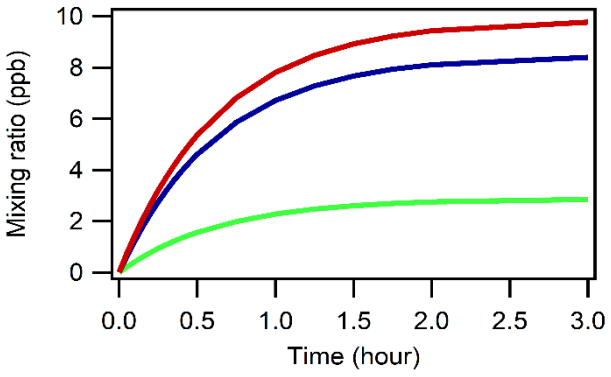

Figure 4: The steady state mixing ratios of formaldehyde released in the room by P1 (blue line), P2 (red line), and P3 (green line), under realistic environmental conditions.

Model calculation shows that the total formaldehyde mixing ratio increases with time reaching a steady state value of 10 ppb for P2, 8 ppb for P1 and 3 ppb for P3 after 3 hours. When the organic paint is replaced by the mineral silicate binder, formaldehyde emissions are calculated to decrease by a factor of 2.7 to 3.4. In comparison, model calculation of formaldehyde emission within a typical furnished room equipped from with coffee table,

dining table, seats and an eco-design sofa were estimated to be 18 ppb [23]. Consequently, such typical living room furnishings appear to be a weak source of formaldehyde in a real-life indoor environment. Under UV irradiation, released mixing ratio of formaldehyde from photocatalytic paint with mineral binder are close to those from reference paints (0.8 ppb)[23].

The emission of formaldehyde induced by different binders is rather low compared to the threshold value of 100 $\mu g\, m^{-3}$ (80 ppb in the U.S standard conditions for temperature and pressure) established by the Indoor Air Quality Guidelines (IAQG)[46] for short term exposure. The mixing ratio of formaldehyde obtained by the P3 is 2.7 to 3.4 times lower than other binders and 27 times lower than IAQG value implying its suitability to not degrade the indoor air quality.

In addition to formaldehyde, P3 reduce considerably the surface emission fluxes for vinyl acetate and ethylbenzene, potential human carcinogens[47].

4. CONCLUSION

Two new binders, organic binder with an acrylic/siloxane and mineral silicate paints were developed and compared with an organic binder (100% acrylic). These paints have been studied using a flow tube reactor coupled with a HS-PTR-MS instrument for real-time monitoring of released VOCs. Surface emission fluxes were measured for seventeen VOCs under given experimental conditions. First, the emissions of selected VOCs by reference paint were compared under "dark" condition and UV irradiation. The emissions fluxes are observed to be similar for the three binders under "dark" conditions and UV irradiation concluding that the composition of the binder does not affect the formation of VOCs. Second, the emissions for photocatalytic paints, containing nano-sized TiO_2 particles, were compared under "dark" conditions. It seems that the mineral binder released more VOCs compared to organic binders, but this difference is relatively low compared to the difference in VOC emissions under UV

irradiation. A comparative study between photocatalytic and reference paints under "dark" conditions revealed that the VOCs emissions are in the same range. The presence of nano-TiO_2 in the binder has a slight effect on VOCs emissions under "dark" conditions. Finally, the comparison of the selected VOCs emissions from acrylic/siloxane and mineral binders and an acrylic binder revealed that the paints with the acrylic/siloxane binder exhibited slightly higher surface emission fluxes as compared with the acrylic binder. Thus, this binder did not improve the properties of the photocatalytic paints with respect to the VOCs emissions.

However, the photocatalytic paints containing the mineral silicate binder exhibited very low VOCs emissions in the presence of UV irradiation. For pentanal and butanoic acid, a decrease in emissions of 88% was observed as compared to the emissions from paints formulated using the acrylic photocatalytic binder. In fact, the use of mineral binder can reduce the quantity of total VOCs emission for about 43% compared to acrylic binder. Moreover, the model simulation of formaldehyde's levels in a real-life indoor environment demonstrated a low formation potential for this compound, implying the lower toxicity of the mineral binder-based paint compared to the all other paints.

For this reason, it can be stated that the development of a mineral binder is an important innovation for reducing the indoor air pollution. In the future, new experiments focused on this binder will be performed to determine its capacity in improving the indoor air quality as a function of time.

ACKNOWLEDGMENTS

The authors acknowledge gratefully LABEX SERENADE (no.ANR-11-LABX-0064) funded by the French National Research Agency (ANR) through the PIA (Programme Investissement d'Avenir).

ASSOCIATED CONTENT

Supporting Information

Notes

The authors declare no competing financial interest.

ACKNOWLEDGMENTS

The authors acknowledge gratefully LABEX SERENADE (no.ANR-11-LABX-0064) funded by the French National Research Agency (ANR) through the PIA (Programme Investissement d'Avenir).

ASSOCIATED CONTENT

Supporting Information

Experimental set up (Figure S1), Values of k, Xr and C (Table S1), Emission surface fluxes for methanol under different conditions (Figure S2), comparison on surface emission fluxes for photocatalytic and reference paints under **"**dark**"** conditions (Figure S3) and surface emission fluxes for different VOCs (Table S2-S7).

Notes

The authors declare no competing financial interest.

REFERENCES

(1) Weschler, C. J. Changes in Indoor Pollutants since the 1950s. *Atmos. Environ.* **2009**, *43* (1), 153–169.

(2) Roberts, J., Nelson, W. . National Human Activity Pattern Survey Data Base. *United States Environ. Prot. Agency* **1995**.

(3) Finlayson-Pitts, B. J.; Pitts, J. N. *Chemistry of the Upper and Lower Atmosphere : Theory, Experiments, and Applications*; Academic Press, 2000.

(4) Bolden, A. L.; Kwiatkowski, C. F.; Colborn, T. New Look at BTEX: Are Ambient Levels a Problem? *Environ. Sci. Technol.* **2015**, *49* (9), 5261–5276.

(5) Salthammer, T.; Mentese, S.; Marutzky, R. Formaldehyde in the Indoor Environment. *Chem. Rev.* **2010**, *110* (4), 2536–2572.

(6) Weschler, C. J.; Nazaroff, W. W. Dermal Uptake of Organic Vapors Commonly Found in Indoor Air. *Environ. Sci. Technol.* **2014**, *48* (2), 1230–1237.

(7) Bekö, G.; Morrison, G.; Weschler, C. J.; Koch, H. M.; Pälmke, C.; Salthammer, T.; Schripp, T.; Toftum, J.; Clausen, G. Measurements of Dermal Uptake of Nicotine Directly from Air and Clothing. *Indoor Air* **2017**, *27* (2), 427–433.

(8) Gligorovski, S.; Li, X.; Herrmann, H. Indoor (Photo)Chemistry in China and Resulting Health Effects. *Environ. Sci. Technol.* **2018**, *52* (19), 10909–10910.

(9) Geiss, O.; Giannopoulos, G.; Tirendi, S.; Barrero-Moreno, J.; Larsen, B. R.; Kotzias, D. The AIRMEX Study - VOC Measurements in Public Buildings and Schools/Kindergartens in Eleven European Cities: Statistical Analysis of the Data. *Atmos. Environ.* **2011**, *45* (22), 3676–3684.

(10) Verriele, M.; Schoemaecker, C.; Hanoune, B.; Leclerc, N.; Germain, S.; Gaudion, V.; Locoge, N. The MERMAID Study: Indoor and Outdoor Average Pollutant Concentrations in 10 Low-Energy School Buildings in France. *Indoor Air* **2015**, *26* (5), 702–713.

(11) Schneider, J.; Matsuoka, M.; Takeuchi, M.; Zhang, J.; Horiuchi, Y.; Anpo, M.; Bahnemann, D. W. Understanding TiO2 Photocatalysis: Mechanisms and Materials.

Chem. Rev. **2014**, *114* (19), 9919–9986.

(12) Hot, J.; Martinez, T.; Wayser, B.; Ringot, E.; Bertron, A. Photocatalytic Degradation of NO/NO2 Gas Injected into a 10-M3 Experimental Chamber. *Environ. Sci. Pollut. Res.* **2017**, *24* (14), 12562–12570.

(13) Dalton, J. S.; Janes, P. A.; Jones, N. G.; Nicholson, J. A.; Hallam, K. R.; Allen, G. C. Photocatalytic Oxidation of NOx Gases Using TiO2: A Surface Spectroscopic Approach. *Environ. Pollut.* **2002**, *120* (2), 415–422.

(14) Devahasdin, S.; Fan, C.; Li, K.; Chen, D. H. TiO2 Photocatalytic Oxidation of Nitric Oxide: Transient Behavior and Reaction Kinetics. *J. Photochem. Photobiol. A Chem.* **2003**, *156* (1), 161–170.

(15) Maggos, T.; Bartzis, J. G.; Leva, P.; Kotzias, D. Application of Photocatalytic Technology for NOx Removal. *Appl. Phys. A* **2007**, *89* (1), 81–84.

(16) Ângelo, J.; Andrade, L.; Madeira, L. M.; Mendes, A. An Overview of Photocatalysis Phenomena Applied to NOx Abatement. *J. Environ. Manage.* **2013**, *129*, 522–539.

(17) Gandolfo, A.; Bartolomei, V.; Gomez Alvarez, E.; Tlili, S.; Gligorovski, S.; Kleffmann, J.; Wortham, H. The Effectiveness of Indoor Photocatalytic Paints on NOx and HONO Levels. *Appl. Catal. B Environ.* **2015**, *166–167*, 84–90.

(18) Wang, S.; Ang, H. M.; Tade, M. O. Volatile Organic Compounds in Indoor Environment and Photocatalytic Oxidation: State of the Art. *Environ. Int.* **2007**, *33* (5), 694–705.

(19) Destaillats, H.; Sleiman, M.; Sullivan, D. P.; Jacquiod, C.; Sablayrolles, J.; Molins, L. Key Parameters Influencing the Performance of Photocatalytic Oxidation (PCO) Air Purification under Realistic Indoor Conditions. *Appl. Catal. B Environ.* **2012**, *128*,

159–170.

(20) Martinez, T.; Bertron, A.; Escadeillas, G.; Ringot, E.; Simon, V. BTEX Abatement by Photocatalytic TiO2-Bearing Coatings Applied to Cement Mortars. *Build. Environ.* **2014**, *71*, 186–192.

(21) Salthammer, T.; Fuhrmann, F. Photocatalytic Surface Reactions on Indoor Wall Paint. *Environ. Sci. Technol.* **2007**, *41* (18), 6573–6578.

(22) Auvinen, J.; Wirtanen, L. The Influence of Photocatalytic Interior Paints on Indoor Air Quality. *Atmos. Environ.* **2008**, *42* (18), 4101–4112.

(23) Gandolfo, A.; Marque, S.; Temime-Roussel, B.; Gemayel, R.; Wortham, H.; Truffier-Boutry, D.; Bartolomei, V.; Gligorovski, S. Unexpectedly High Levels of Organic Compounds Released by Indoor Photocatalytic Paints. *Environ. Sci. Technol.* **2018**, *52* (19), 11328–11337.

(24) George, C.; Strekowski, R. S.; Kleffmann, J.; Stemmler, K.; Ammann, M. Photoenhanced Uptake of Gaseous NO2 on Solid Organic Compounds: A Photochemical Source of HONO? *Faraday Discuss.* **2005**, *130* (0), 195–210.

(25) Hanson, D. R.; Ravishankara, A. R. Uptake of Hydrochloric Acid and Hypochlorous Acid onto Sulfuric Acid: Solubilities, Diffusivities, and Reaction. *J. Phys. Chem.* **1993**, *97* (47), 12309–12319.

(26) Bartolomei, V.; Sörgel, M.; Gligorovski, S.; Alvarez, E. G.; Gandolfo, A.; Strekowski, R.; Quivet, E.; Held, A.; Zetzsch, C.; Wortham, H. Formation of Indoor Nitrous Acid (HONO) by Light-Induced NO2 Heterogeneous Reactions with White Wall Paint. *Environ. Sci. Pollut. Res.* **2014**, *21* (15), 9259–9269.

(27) de Gouw, J.; Warneke, C. Measurements of Volatile Organic Compounds in the

Earth's Atmosphere Using Proton- transfer- reaction Mass Spectrometry. *Mass Spectrom. Rev.* **2006**, *26* (2), 223–257.

(28) Hayeck, N.; Temime-Roussel, B.; Gligorovski, S.; Mizzi, A.; Gemayel, R.; Tlili, S.; Maillot, P.; Pic, N.; Vitrani, T.; Poulet, I.; et al. Monitoring of Organic Contamination in the Ambient Air of Microelectronic Clean Room by Proton-Transfer Reaction/Time-of-Flight/Mass Spectrometry (PTR–ToF–MS). *Int. J. Mass Spectrom.* **2015**, *392* (Supplement C), 102–110.

(29) de Gouw, J. A.; Goldan, P. D.; Warneke, C.; Kuster, W. C.; Roberts, J. M.; Marchewka, M.; Bertman, S. B.; Pszenny, A. A. P.; Keene, W. C. Validation of Proton Transfer Reaction-Mass Spectrometry (PTR-MS) Measurements of Gas-Phase Organic Compounds in the Atmosphere during the New England Air Quality Study (NEAQS) in 2002. *J. Geophys. Res. Atmos.* **2003**, *108* (D21).

(30) Cappellin, L.; Karl, T.; Probst, M.; Ismailova, O.; Winkler, P. M.; Soukoulis, C.; Aprea, E.; Märk, T. D.; Gasperi, F.; Biasioli, F. On Quantitative Determination of Volatile Organic Compound Concentrations Using Proton Transfer Reaction Time-of-Flight Mass Spectrometry. *Environ. Sci. Technol.* **2012**, *46* (4), 2283–2290.

(31) Zhao, J.; Zhang, R. Proton Transfer Reaction Rate Constants between Hydronium Ion (H3O+) and Volatile Organic Compounds. *Atmos. Environ.* **2004**, *38* (14), 2177–2185.

(32) Vlasenko, A.; Macdonald, A. M.; Sjostedt, S. J.; Abbatt, J. P. D. Formaldehyde Measurements by Proton Transfer Reaction – Mass Spectrometry (PTR-MS): Correction for Humidity Effects. *Atmos. Meas. Tech.* **2010**, *3* (4), 1055–1062.

(33) Manoukian, A.; Quivet, E.; Temime-Roussel, B.; Nicolas, M.; Maupetit, F.; Wortham, H. Emission Characteristics of Air Pollutants from Incense and Candle Burning in Indoor Atmospheres. *Environ. Sci. Pollut. Res.* **2013**, *20* (7), 4659–4670.

(34) Karl, T. G.; Christian, T. J.; Yokelson, R. J.; Artaxo, P.; Hao, W. M.; Guenther, A. The Tropical Forest and Fire Emissions Experiment: Method Evaluation of Volatile Organic Compound Emissions Measured by PTR-MS, FTIR, and GC from Tropical Biomass Burning. *Atmos. Chem. Phys.* **2007**, *7* (22), 5883–5897.

(35) Hartungen, E. von; Wisthaler, A.; Mikoviny, T.; Jaksch, D.; Boscaini, E.; Dunphy, P. J.; Märk, T. D. Proton-Transfer-Reaction Mass Spectrometry (PTR-MS) of Carboxylic Acids: Determination of Henry's Law Constants and Axillary Odour Investigations. *Int. J. Mass Spectrom.* **2004**, *239* (2), 243–248.

(36) Jobson, B. T.; Alexander, M. L.; Maupin, G. D.; Muntean, G. G. On-Line Analysis of Organic Compounds in Diesel Exhaust Using a Proton Transfer Reaction Mass Spectrometer (PTR-MS). *Int. J. Mass Spectrom.* **2005**, *245* (1), 78–89.

(37) Katsoyiannis, A.; Leva, P.; Kotzias, D. VOC and Carbonyl Emissions from Carpets: A Comparative Study Using Four Types of Environmental Chambers. *J. Hazard. Mater.* **2008**, *152* (2), 669–676.

(38) Järnström, H.; Saarela, K.; Kalliokoski, P.; Pasanen, A.-L. Reference Values for Structure Emissions Measured on Site in New Residential Buildings in Finland. *Atmos. Environ.* **2007**, *41* (11), 2290–2302.

(39) Wolkoff, P. Volatile Organic Compounds Sources, Measurements, Emissions, and the Impact on Indoor Air Quality. *Indoor Air* **1995**, *5* (S3), 5–73.

(40) Hodgson, A.; Beal, D.; McIlvaine, J. Sources of Formaldehyde, Other Aldehydes and Terpenes in a New Manufactured House. *Indoor Air* **2002**, *12* (4), 235–242.

(41) Guo, H.; Kwok, N. H.; Cheng, H. R.; Lee, S. C.; Hung, W. T.; Li, Y. S. Formaldehyde and Volatile Organic Compounds in Hong Kong Homes: Concentrations and Impact

Factors. *Indoor Air* **2009**, *19* (3), 206–217.

(42) Tanaka-Kagawa, T.; Furuta, M.; Shibatsuji, M.; Jinno, H.; Nishimura, T. [Volatile organic compounds (VOCs) emitted from large furniture]. *Kokuritsu Iyakuhin Shokuhin Eisei Kenkyusho. Hokoku* **2011**, No. 129, 76–85.

(43) Kelly, T. J.; Smith, D. L.; Satola, J. Emission Rates of Formaldehyde from Materials and Consumer Products Found in California Homes. *Environ. Sci. Technol.* **1999**, *33* (1), 81–88.

(44) Gómez Alvarez, E.; Sörgel, M.; Gligorovski, S.; Bassil, S.; Bartolomei, V.; Coulomb, B.; Zetzsch, C.; Wortham, H. Light-Induced Nitrous Acid (HONO) Production from NO2 Heterogeneous Reactions on Household Chemicals. *Atmos. Environ.* **2014**, *95*, 391–399.

(45) Wallace, L. A.; Emmerich, S. J.; Howard-Reed, C. Continuous Measurements of Air Change Rates in an Occupied House for 1 Year: The Effect of Temperature, Wind, Fans, and Windows*. *J. Expo. Anal. Environ. Epidemiol.* **2002**, *12*, 296.

(46) Nielsen, G. D.; Larsen, S. T.; Wolkoff, P. Re-Evaluation of the WHO (2010) Formaldehyde Indoor Air Quality Guideline for Cancer Risk Assessment. *Arch. Toxicol.* **2017**, *91* (1), 35–61.

(47) US EPA, O. Dose-Response Assessment for Assessing Health Risks Associated With Exposure to Hazardous Air Pollutants.